ARE THERE IRON OXIDES IN LUNAR BASALTS? J. Jung[1] (jiinjung@stanford.edu), S. M. Tikoo[1,2], D. Burns[2], S. Channa[3], [1]Dept. of Geophysics, Stanford University, Stanford, CA 94305; [2]Dept. of Earth and Planetary Sciences, Stanford University, Stanford, CA 94305; [3]Dept. of Physics, Stanford University, Stanford, CA 94305.

Introduction: The Moon is considered to have a reducing environment, which results in the presence of metallic iron phases within igneous rocks instead of iron oxides (e.g., magnetite and hematite) commonly occurring on Earth [1-4]. During primary cooling, the body-centered cubic FeNi alloys kamacite (α-$Fe_{1-x}Ni_x$ for x < ~0.05) and martensite (α_2-$Fe_{1-x}Ni_x$ for ~0.05 < x < ~0.25) formed in lunar mare basalts. These FeNi grains are typically either embedded within troilite (FeS) in a eutectic assemblage or associated with chromite ($FeCr_2O_4$) [5]. However, other occurrences of FeNi grains (interstitial, isolated within mesostasis glass, inclusions within silicates) may also occur. Additionally, space weathering processes can create nanophase iron particles ($npFe^0$) on the lunar surface [6].

Recent studies have discovered the presence of ferric iron and magnetite in regolith breccias [7] and lunar soils [8]. Their origins may have been attributed to impact-related secondary processes, such as magnetite formation by oxidizing agents from exogenic sources [7] or formation under different oxygen fugacity conditions [8]. Intriguingly, one Apollo-era paleomagnetic study claimed to have potentially identified magnetite in mare basalts from observing a low-temperature magnetic transition [9] known as the Verwey transition at ~120 K [10]. However, this finding was not widely followed up on as magnetite had not yet been identified by petrologists. It was also posited that the low-temperature magnetic behavior could be attributed to chromite [11]. In this study, we use detailed electron microprobe analyses and rock magnetic measurements to investigate the presence/role of iron oxides as magnetic carriers in various mare basalts.

Methods: We conducted a detailed study of high-K ilmenite basalt 10071, which contains intergrown troilite and kamacite (**Fig. 1a**). We employed scanning electron microscopy with energy dispersive x-ray spectroscopy (SEM/EDS) as well as electron probe microanalysis (EPMA) on a thin section. Wavelength-dispersive spectroscopy (WDS) scans were performed at 7 keV using a focused electron beam and a probe current of 20 nA. Pure Fe metal and magnetite standards were also measured for reference.

To investigate the magnetic properties of potential carriers, we performed first-order reversal curve (FORC) analyses and examined low-temperature magnetic behaviors by Magnetic Property Measurement System (MPMS) experiments. Apollo samples with different FeNi occurrences (i.e., kamacite associated with troilite for 10003, 10020, 10044, 10069 and FeNi alloys associated with chromite for 10020, 12022, and 15597) were also measured in order to identify potential magnetic phases at low temperatures such as chromite, ulvospinel, ilmenite, and troilite. For each sample, we conducted measurements of both field-cooled magnetization (FC) in a 2T field and zero field-cooled magnetization (ZFC), as well as the cooling and heating behaviors of room-temperature saturated isothermal remanent magnetization (RTsIRM).

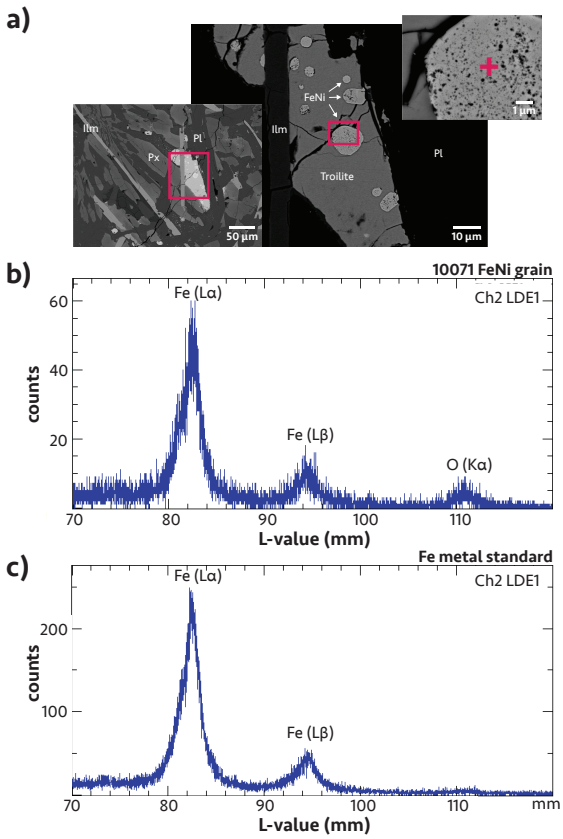

Fig. 1. a) BSE images of FeNi alloys embedded in the troilite phase for sample 10071. Close-up look of the target location (red boxes) from left to right. **b)** WDS spectra at 7 keV for the target FeNi grain (red cross area in a) and **c)** Fe standard for comparison. Pl = Plagioclase, Px = Pyroxene, Ilm = ilmenite

Results: We targeted kamacite grains within sample 10071 for WDS scans because EDS elemental mapping showed that the metallic phase contained higher oxygen counts than surrounding troilite phases. WDS scans of the metallic phase (**Fig. 1b**) show distinct peaks for Fe (Lα and Lβ) and oxygen (Kα), with preliminary quantitative analyses yielding oxygen concentration

between 3 and 4 wt. %. In contrast, WDS scans collected on an Fe-metal standard analyzed during the same session at similar analytical conditions did not show a pronounced oxygen peak (**Fig. 1c**). Some Fe metallic phases from other FeNi-troilite assemblages in the same sample showed a considerably smaller oxygen peak. Ongoing work will explore whether these smaller oxygen peaks could be due to surface oxidation.

MPMS results for sample 10071 showed a phase transition at ~120K in FC, ZFC, and RTsIRM curves (**Fig. 2a**). One possible magnetic carrier is chromite (which has three possible transitions at 37K, 69K, and 124K) [12, 13]. However, we did not observe chromite in this sample. We also found that the low-temperature behaviors of known chromite-bearing lunar basalts (e.g., 10020, 12022, 15597) differed from those of troilite-bearing samples similar to 10071 (e.g., 10003, 10044, 10069). The Curie temperature of ulvospinel is ~115K [14], but this mineral is absent in Apollo 11 high-K basalts [15]. An increase in magnetization at ~120 K suspiciously resembles the magnetite Verwey transition [10]. If this is the case, $\delta_{FC}/\delta_{ZFC} > 1$ below the transition indicates that the magnetite grains would likely be single domain (SD) [16]. Another notable feature is a phase transition at around ~50 K from FC and RTsIRM curves. This might be consistent with the Néel transition of troilite at ~ 60 K [17] or ilmenite at ~ 65 K [18].

In the FORC diagram (**Fig. 2b**), the cluster at $B_c = 0$ spreading along the B_u axis indicates the presence of multidomain and pseudo-single domain-like grains, which is consistent with the kamacite sizes observed from optical microscopy. A horizontal ridge extending to high coercivity (>100 mT) along $H_u = 0$ indicates a population of SD grains within the sample. This requires nm-size grains (e.g., ~10-50 nm threshold size for Fe particles [19] and magnetite [20]), which are too small to be measured via EPMA.

Discussion: We studied the magnetic properties of Apollo sample 10071. Our electron microscope results revealed slight oxygens in Fe grains in troilite. MPMS data show a magnetic transition at ~50K (broadly consistent with the presence of troilite and ilmenite) and ~120K. The latter transition could potentially be a signature of SD magnetite. FORC data also indicate the presence of SD magnetic fractions. Identifying this magnetic carrier and determining how it formed will help to understand past lunar environments as well as magnetic carriers in lunar paleomagnetism. Future analyses, such as transmission electron microscopy (TEM), are required to validate our results.

Acknowledgments: We thank R. Ziegler and J. Gross, CAPTEM, and the Lunar Receiving Laboratory at Johnson Space Center for allocating and preparing our samples. We also thank the Institute of Rock Magnetism (IRM) at the University of Minnesota, especially P. Solheid, for assistance with FORC and MPMS measurements. This research was supported by a NASA FINESST grant under award number 80NSSC21K1541.

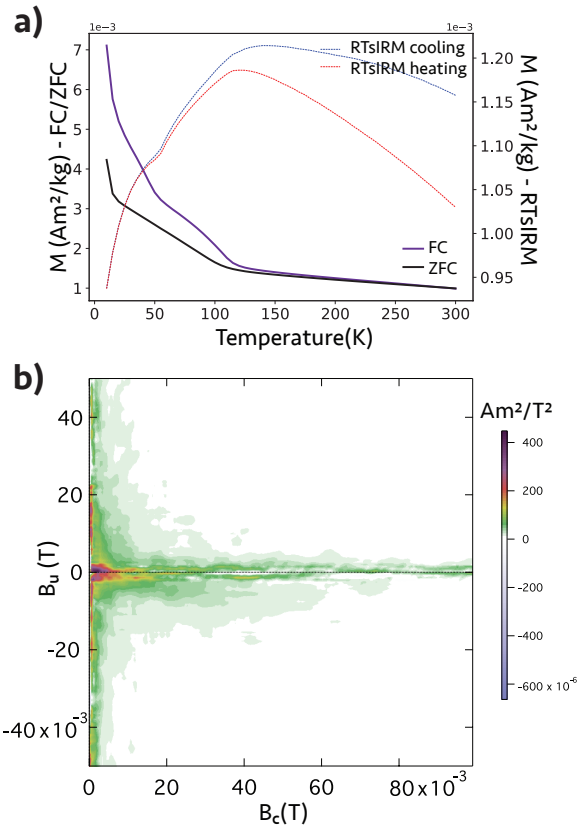

Fig. 2. a) Temperature vs moment for sample 10071 acquired by MPMS experiments. Note that scales are different for FC/ZFC curves (left vertical axis) and RTsIRM curves (right vertical axis). **b)** FORC diagram for the sample 10071. FORCs distribution was calculated with N = 268 FORCs with 5 stackings using FORCinel software [21].

References: [1] Sato M. et al., (1973), *Proc. Lunar Sci. Conf. 4th,* 1061-1079. [2] Sato M. (1976) *Proc. Lunar Sci. Conf. 7th,* 1323-1344. *[3] Haggerty S. E. (1978) GRL*, 5, 443-446. [4] Tikoo S. M, and A. J. Evans., (2021) *Annu. Rev. Earth. Planet. Sci., 50:1*, 99-122. [5] Skinner B., (1970) *Sci., 167*, 3918. [6] Pieters C. M. and S. K. Noble (2016) *JGR Planets,* 121, 1865-1884. [7] Guo Z. et al., (2022) *Nat. commun., 13*, 7177. [8] Joy K. H. et al., (2015) *Meteorit. Plant. Sci. 50,* 1157-1172. [9] Runcorn S. K. et al., (1971) *Proc. R. Soc. Lond., 325,* 157-173. [10] Verwey E. J. W. (1939) *Nat., 44,* 327-328. [11] Fuller M. (1974) *Rev. Geophys. and Space Phys.,12*, 23-70. [12] Klemme S. et al., (2000) *Ame Min*, *85*, 1686-1693. [13] Gattacceca J. et al., (2011) *GRL, 38*, L10203. [14] Readman R. W. (1978) *Phys. Earth Planet. Inter. 16,* 196-199. [15] Warner R. D. et al., (1978) *Ame Min*, *63*, 1209-1224. [16] Moskowitz B. M. et al., (1993) *LPSC, 120,* 283-300. [17] Kohout T. A. et al., (2007) *EPSL, 261*, 131-151. [18] Senftle P. A. et al., (1975) *EPSL, 26,* 377-386. [19] Muxworthy A. R. and W. Williams (2015) *Geophys. J. Int., 202*, 578-583. [20] Butler R. F. and S. K. Banerjee (1975) *JGR, 80*, 29. [21] Harrison R. J and J. M. Feinberg (2008) *Geochem. Geophys. Geosystems.,9,* Q05016.